

Covalent Mucin Coatings Form Stable Anti-Biofouling Layers on a Broad Range of Medical Polymer Materials

Benjamin Winkeljann, Maria G. Bauer, Matthias Marczynski, Theresa Rauh, Stephan A. Sieber, and Oliver Lieleg*

Approximately 10% of all hospital patients contract infections from temporary clinical implants such as urinal and vascular catheters or tracheal tubes. The ensuing complications reach from patient inconvenience and tissue inflammation to severe, life threatening complications such as pneumonia or bacteremia. All these device-associated nosocomial infections have the same origin: biofouling, i.e., the unwanted deposition of proteins, bacteria, and cells onto the device. To date, most strategies to overcome these problems are device specific, which results in high development efforts and costs. Here, it is demonstrated how one and the same coupling mechanism can be used to create a covalent antifouling coating employing mucin glycoproteins on multiple materials: with this method, a stable mucin layer can be generated on a broad range of polymer materials which are frequently used in medical engineering. It is shown that the mucin coating exhibits excellent stability against mechanical, thermal, and chemical challenges and reduces protein adsorption as well as prokaryotic and eukaryotic cell adhesion. Thus, the coating mechanism described here introduces a promising strategy to overcome biofouling issues on a broad range of medical devices.

important: e.g., the material has to resist biofouling events and/or needs to be compatible with cells/tissues or body fluids. Especially biofouling on medical devices is a major problem, as it is responsible for a huge amount of nosocomial infections.

Thus, during the past decades, different types of surface functionalizations and coatings^[1] have been investigated which aim at preventing (or at least minimizing) problems that arise from using a foreign, artificial material in or on the human body. For instance, macromolecular coatings have been introduced to improve the biocompatibility of synthetic materials thus reducing foreign body responses. Examples include coatings that reduce the adsorption of proteins,^[2] cells,^[3] and pathogens^[4] and coatings that reduce mechanical damage on soft tissues by generating a lubricious, slippery surface.^[5] For each of those coatings it is important to guarantee a good stability of the surface modification; the uncontrolled

1. Introduction


When a medical device, i.e., a foreign, artificial material, comes into contact with the human body, there are several issues that need to be considered: As a basic requirement, the material needs to be formed in a certain shape and has to possess dedicated mechanical properties to fulfill its desired function. Moreover, depending on the type of application, several other properties are

liberation of molecules from the material coating into the human body may induce unwanted/unforeseeable side effects. This concern limits the use of synthetic polymers in clinical applications as long as the interactions of those synthetic molecules with the human body are not fully understood. Biomacromolecules, which are natural products, typically offer the advantage of excellent biocompatibility. Thus, they have gained increased attention as potential components for coatings. However, the application of such biopolymers as components of medical product coatings remains challenging as biological macromolecules can be sensitive to mechanical or chemical challenges including quick degradation.^[6]

Recently, mucin glycoproteins have been tested as coatings to suppress biofouling events.^[7] Indeed, mucin coated surfaces not only reduce the adsorption of small proteins; they also decrease the attachment of bacteria such as *Streptococcus pneumoniae* and *Staphylococcus aureus*,^[8] and they can improve the hemocompatibility of medical devices.^[9] Mucins are a group of large glycoproteins with molecular weights of up to a few MDa.^[10] They are the main component of mucus, the transparent hydrogel covering all wet epithelia in the human body, including the corneal surface,^[11] the gastrointestinal tract^[12] and the female reproductive system.^[13] One of the physiological functions of mucins is to protect the underlying epithelial cells from dehydration. Furthermore, mucus has unique selective properties that, on the one hand, allow nutrients to pass but, on the other hand, trap or repel pathogens such as viruses or bacteria.^[14] Owing to their

B. Winkeljann, M. G. Bauer, M. Marczynski, Prof. O. Lieleg
Department of Mechanical Engineering and Munich School
of Bioengineering
Technical University of Munich
Boltzmannstraße 11, 85748 Garching, Germany
E-mail: oliver.lieleg@tum.de

T. Rauh, Prof. S. A. Sieber
Department of Chemistry
Chair of Organic Chemistry II
Technical University of Munich
Lichtenbergstraße 4, 85748 Garching, Germany

 The ORCID identification number(s) for the author(s) of this article can be found under <https://doi.org/10.1002/admi.201902069>.

© 2020 The Authors. Published by WILEY-VCH Verlag GmbH & Co. KGaA, Weinheim. This is an open access article under the terms of the Creative Commons Attribution License, which permits use, distribution and reproduction in any medium, provided the original work is properly cited.

DOI: 10.1002/admi.201902069

ability to bind many water molecules^[15] and to adsorb to various surfaces,^[10,16] mucins also serve as excellent lubricants and thus protect the sensitive cellular surface from mechanical damage.

Mucin solutions have not only been proven to efficiently lubricate physiological systems but can also reduce friction and wear formation in technical material pairings^[17] or in hybrid systems, i.e., when artificial materials come in contact with a biological surface.^[18] In certain cases, even simple mucin coatings achieved by passive adsorption can be an effective tool in reducing mechanical damage caused by medical devices, e.g., when contact lenses rub against corneal tissue.^[5c] For other medical applications, e.g., catheters or ventilation tubes, a coating via passive adsorption is probably not stable enough to withstand the large mechanical load occurring during the insertion/extraction of the medical device. Yet, a stable coating is indispensable for a medical application: even small, local damages would be weak spots for initial stages of biofouling. Covalent mucin coatings have, however, only rarely been generated in the past,^[9,19] and their stability and anti-biofouling properties still need to be evaluated in detail.

We here describe a coating protocol, which allows for covalently attaching mucin glycoproteins to a broad range of medical polymer materials without the need to change the coupling chemistry. We demonstrate, that these mucin coatings are stable toward different environmental conditions such as increased temperature, chemicals, pH variations, or mechanical stress. Finally, we show, that our mucin coatings efficiently reduce different types of fouling events, i.e., the adsorption of small proteins, particles, and also the attachment of clinically relevant pathogens such as *Pseudomonas aeruginosa*, *Streptococcus pyogenes*, and *S. aureus* as well as eukaryotic cells.

2. Experimental Section

2.1. Mucin Purification

Porcine gastric mucin MUC5AC was purified manually as described previously.^[20] In brief, mucus was obtained from gently rinsed pig stomachs by manual scraping the inner surface of the gastric tissue. The collected mucus was diluted 5-fold in 10×10^{-3} M sodium phosphate buffer (pH = 7.0) containing 170×10^{-3} M NaCl and 0.04% (w/v) sodium azide (Carl Roth, Karlsruhe, Germany) and stirred at 4 °C overnight. Cellular debris was removed via two centrifugation steps (first run: $8300 \times g$ at 4 °C for 30 min; second run: $15\,000 \times g$ at 4 °C for 45 min) and a final ultracentrifugation step ($150\,000 \times g$ at 4 °C for 1 h). Subsequently, the mucins were separated from other macromolecules by size exclusion chromatography using an ÄKTA purifier system (GE Healthcare, Munich, Germany) and an XK50/100 column packed with Sepharose 6FF. The obtained mucin fractions were pooled, dialyzed against ultrapure water and concentrated by cross-flow filtration (MWCO: 100 kDa; Xampler Ultrafiltration Cartridge, GE Healthcare). The concentrate was then lyophilized and stored at -80 °C until further use.

2.2. Fluorescence Labelling of Proteins

To allow for a visualization of either the mucin coating or the adsorption of small proteins (here bovine serum albumin (BSA)

and lysozyme were used as model proteins), these proteins were labelled with a green fluorescing dye (ATTO488 carboxy modified, ATTO-TEC GmbH, Siegen, Germany). The carboxy modified ATTO dye was coupled to the proteins via carbodiimide coupling. Therefore, the dye was first diluted to a concentration of $c_{\text{ATTO}} = 1.0 \text{ mg mL}^{-1}$ in MES buffer (10×10^{-3} M, pH = 5) at a final volume of 1 mL. Afterward 5×10^{-3} M EDC and 10×10^{-3} M sulfo-NHS were added to this solution and it was allowed to incubate light excluded for 3 h at room temperature (RT = 21 °C). This prolonged incubation time ensured that remaining free EDC was hydrolyzed before mucin was added to avoid crosslinking of protein molecules. In parallel, 40 mg of either purified mucin, BSA (Albumin Fraction V, Carl Roth) or lysozyme (Sigma Aldrich) were dissolved in 19 mL PBS (10×10^{-3} M, pH = 7). Then, both solutions were mixed thoroughly and again allowed to react for 3 h at RT. To remove unbound dye molecules the mixture was dialyzed (MWCO = 300 kDa for mucin, MWCO = 6–8 kDa for BSA and lysozyme) against ultrapure water. The solution was then lyophilized and stored at -80 °C until further use.

2.3. Sample Preparation

PDMS cylinders were prepared by mixing PDMS (SYLGARD 184, Dow Corning, Midland, U.S.A.) in a 10:1 ratio with the curing agent and exposing the mixture to vacuum for 1 h to remove air bubbles before curing at 80 °C for 1 h. Since other studies indicated that there might be unreacted low molecular weight residues left after curing the PDMS,^[21] the samples were further tempered at 100 °C for 2 h. Prior to surface modification, the specimens were cleaned with 80% ethanol and ultrapure water.

2.4. Coating Process

The coupling reaction was performed as described previously.^[19] Briefly, the PDMS samples were treated with O₂ plasma at 0.4 mbar pressure and an intensity of 30 W for 90 s. The plasma treatment replaces the methoxy groups on the polymer surface with hydroxyl groups which enable a covalent attachment of silane molecules. The silane was used as a coupling agent to further allow for linking the porcine gastric mucin to the surface via carbodiimide coupling.

Thus, N-[3-Trimethoxysilyl]propyl]ethylenediamine triacetic acid trisodium salt (TMS-EDTA, abcr, Karlsruhe, Germany) was used here, which was carrying three carboxy groups on the other end. TMS-EDTA was diluted to a final concentration of 0.1% (w/v) in 10×10^{-3} M sodium acetate buffer (pH = 4.5). The activated PDMS pins were then incubated in the silane solution for 5 h at 60 °C. Afterward the samples were washed in 96% ethanol (Carl Roth) for 1 h to remove unbound residues before they were placed in the oven at 110 °C for another 60 min to stabilize the bond between the PDMS and the silane. In a next step, the carboxyl groups of the silane were activated. Therefore, the pins were immersed in 100×10^{-3} M MES buffer (pH = 5.0) containing 5×10^{-3} M 1-ethyl-3-(3-dimethylaminopropyl)-carbodiimid-hydrochlorid (EDC, Carl Roth) and 5×10^{-3} M

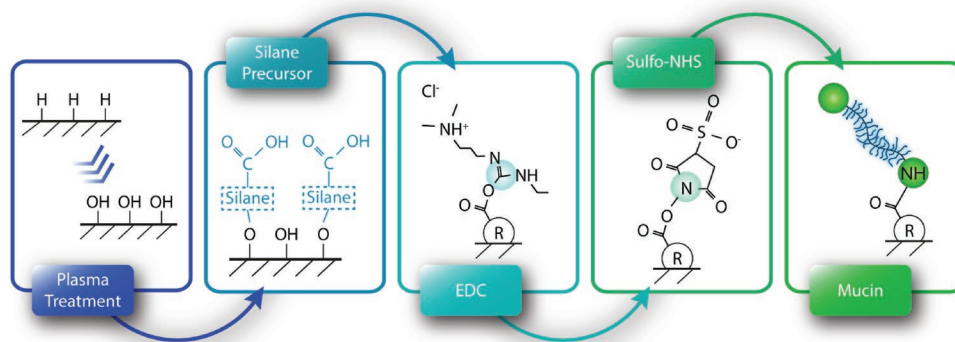


Figure 1. Schematic representation of the coating process. To functionalize PDMS, its surface is first activated with O₂-plasma and then precoated with a silane-based precursor. Afterward, porcine gastric mucin can be covalently linked to the precoated surface by means of carbodiimide coupling.

N-Hydroxysulfosuccinimide (sulfo-NHS, abcr) for 30 min at RT. Afterward the EDC-NHS solution was replaced by phosphate buffered saline (pH = 7.4, Lonza, Verviers, Belgium) containing 0.1% (w/v) of purified mucin and stored overnight at 4 °C. Amine groups of the mucin protein core then react with the EDC activated groups of the silane to form a stable covalent bond (Figure 1).

2.5. ELISA

To test the coated samples for presence of mucin on the surface, indirect enzyme linked immunosorbent assays (ELISA) were performed. Therefore, each sample was placed into a well of a 96 well cell culture plate and rinsed with PBS-Tween (containing 1 mg mL⁻¹ Tween 20, Carl Roth, pH = 7.4) three times. Afterward, all samples were incubated in blocking buffer (comprising 5% (w/v) milk powder dissolved in PBS-Tween) at 4 °C overnight. For the following steps of the ELISA protocol, an empty well was filled with blocking buffer for each sample.

On the next day, the blocked wells and the wells containing the PDMS samples were again rinsed with PBS-Tween. Then, each sample was transferred into one of the blocked wells. Afterward, the samples were incubated with a primary antibody (200 µL per well) for 1 h while shaking (Promax 1020, Heidolph Instruments GmbH & Co. KG, Schwabach, Germany). For this step, a specific antibody for MUC5AC detection (ABIN966608, antibodies-online GmbH, Aachen, Germany) was used. The mucin antibody was diluted 1:400 in blocking buffer. After incubation for 1 h, the wells were rinsed again with PBS-Tween. A second antibody staining was then performed using a horse radish peroxidase (HRP) conjugated goat anti-mouse IgG antibody (ABIN237501, antibodies-online GmbH). This secondary antibody was diluted 1:5000 in blocking buffer. Incubation was allowed to take place for 2 h on a shaker at RT. Afterward, the samples were washed in pure PBS (since Tween tends to interfere with the solutions used for the following steps). After washing the wells, 100 µL of QuantaRed Working Solution were added into each well. The QuantaRed Working Solution consists of 50 parts QuantaRed Enhancer Solution, 50 parts QuantaRed Stable Peroxide and one part of QuantaRed ADHP Concentrate (QuantaRed Enhanced Chemifluorescent

HRP Substrate Kit 15 159, Thermo Fisher Scientific, Waltham, Massachusetts, USA). Since the working solution was light sensitive, direct light contact was avoided.

After 30 min of incubation at RT, the peroxidase activity was stopped by adding 20 µL of QuantaRed Stop Solution to each well. The plate was incubated on the shaker again for 30 s before samples were removed from the wells and fluorescence of the converted substrate was measured with a multilabel plate reader (Viktor3, PerkinElmer, Inc., Massachusetts, USA). Fluorescence was measured at a wavelength of 570 nm using a data acquisition time of 0.1 s.

2.6. Mechanical Stability

To compare the mechanical stability of passively adsorbed and covalently attached mucin layers on a PDMS surface PDMS pins were first exposed to mechanical stress in a rotational tribology setup and afterward analyzed via ELISA. Tribological treatment was performed on a commercial shear rheometer (MCR 302, Anton Paar, Graz, Austria) that was equipped with a tribology unit (T-PTD 200, Anton Paar) and a ball-on-cylinder geometry (Figure 3a). As a friction partner in the tribology setup, steel spheres with a diameter of 12.7 mm (1.4301, Kugel Pompel, Vienna, Austria) were chosen. Measurements were performed at a constant normal load of $F_N = 6$ N, which resulted in an average contact pressure of ≈ 0.31 MPa.^[19] The speed dependent friction behavior was evaluated by performing three logarithmic speed ramps from ≈ 700 to 0.001 mm s⁻¹. Before the first measuring point, the system was allowed to stabilize at the highest rotational speed for 30 s. In each measurement, 600 µL of HEPES buffer (20×10^{-3} M, pH = 7.0) were used as a lubricant. For ELISA tests, the pins were carefully removed from the sample holder after the treatment and rinsed with distilled water. From the treated PDMS pins, a small cylinder ($d = 2$ mm) was punched out from the center, i.e., the area that comes in contact with the rotating steel sphere during the tribological treatment, and an ELISA test was performed with this small cylindrical sample as described above. This procedure reduces the influence of the background fluorescence signal arising from untreated pin surfaces. As a control, pins, which had not been exposed to mechanical stress were treated the same way.

The mechanical stability of coatings on PMMA specimens was tested using an ultrasonic treatment. Therefore, small PMMA pieces (4 mm x 4 mm x 1 mm) were prepared and either coated via passive adsorption or using the covalent coupling process as described above. Then, the samples were immersed into Millipore water and exposed to ultrasonic treatment (5510E-MTH, Branson Ultrasonic Corporation, Danbury, CT, USA) for 1 h. Afterward, they were rinsed in Millipore water and the amount of surface bound mucin was analyzed via ELISA. Control specimens were coated in a similar way but without the exposure to ultrasonic treatment.

2.7. Chemical Stability

To analyze the chemical stability of the mucin coating, samples were incubated in different solutions, each containing one of the following ingredients: 96% ethanol, 1 M guanidium thiocyanate (GTC, Carl Roth), 1 M sodium chloride (Carl Roth) or 6 M urea (Sigma Aldrich), all dissolved in PBS. Furthermore, the stability of the coatings toward different pH conditions was tested by incubation in either 1 M formic acid (pH = 1.5, Carl Roth), 1×10^{-6} M sodium hydroxide (pH = 8.0, Sigma Aldrich) or 1 M sodium hydroxide (pH = 13.5) solution. Finally, also a set of different enzymes was tested: trypsin (0.1 mg mL⁻¹, dissolved in PBS, pH = 7.4, Sigma Aldrich), protease Type XIV (0.2 mg mL⁻¹, dissolved in 10×10^{-3} M sodium acetate containing 5×10^{-3} M calcium acetate, pH = 7.5, Sigma Aldrich), proteinase K (0.1 mg mL⁻¹, dissolved in 0.5% SDS containing 2.5×10^{-3} M calcium chloride, pH = 8, Sigma Aldrich) and pepsin (4.0 mg mL⁻¹, dissolved in 100×10^{-3} M HCl, pH = 1, Sigma Aldrich). To mimic physiological conditions all stability tests were performed by incubating the coated samples at 37 °C overnight.

Subsequently, all samples were thoroughly rinsed thrice: first with Millipore water, then with 80% ethanol and again with Millipore water. This ensures that all residues of the enzyme solution and unbound mucin proteins were removed. Control samples underwent the same mechanical and thermal conditions; however, they were immersed into simple PBS lacking any enzyme. The amount of remaining mucin in the coating was then assessed via ELISA, as described above.

2.8. Contact Angle Measurements

To determine the surface polarities of the different synthetic polymer materials before and after the mucin coating, contact angle measurements were conducted. Therefore, samples were first cleaned with 80% ethanol and Millipore water. After drying the samples, a droplet of 8 µL Millipore water was placed onto each sample, and a transversal image of the liquid–solid interface was captured using a high-resolution camera (Point Gray Research, Richmond, Canada). Then, the static contact angle value was determined using the software Image J and the “drop snake” plug-in.

2.9. Protein and Particle Adsorption

Adsorption tests were conducted on samples inspired by so called Janus's particles: For the experiments conducted here,

cuboid samples (2 mm x 4 mm x 18 mm) were separated into three different zones each of which was coated differently. The top area remained uncoated, the central area was precoated with the silane precursor, and the bottom area received the full two-layer coating, i.e., precursor and mucin. To test the antiadhesive properties of the coatings, a set of 5 to 7 Janus inspired plates (JIPs) was inserted into a 5 mL laboratory tube filled up with a 10×10^{-3} M HEPES solution containing either 0.1% (w/v) of fluorescent proteins (BSA, lysozyme) or red fluorescent polystyrene (PS) nanoparticles ($d = 300$ nm, either aminated or carboxylated, Invitrogen, Thermo Fisher Scientific). The ζ -potential of the PS nanoparticles was determined with dynamic light scattering using a Zetasizer Nano ZS (Malvern Instruments, Herrenberg, Germany) at a concentration of 1:1000 in 10×10^{-3} M HEPES buffer (pH = 7.0).

While protected from light, the tube containing the JIPs was placed onto an orbital shaker (10–15 rpm, Polymax 2040, Heidolph Instruments GmbH & CO. KG, Schwabach, Germany) for 20–30 min. After this incubation, the samples were rinsed with Millipore water. The JIPs were placed onto a microscope slide and left to dry for 2–3 min. Once the JIPs were completely dry, images were acquired on a fluorescent microscope (Axioskop 2 MAT mot, Carl Zeiss AG, Oberkochen, Germany) equipped with a mercury arc lamp as a light source (HBO 103 W/2, Osram, Munich, Germany) and a digital camera (C10600 ORCA-R2, Hamamatsu Photonics Europe GmbH, Herrsching, Germany). For images of samples incubated with nanoparticles (NPs), 10× magnification and an appropriate filter set (excitation: BP 546/12 nm, filter block: 580 nm, emission: LP 590 nm) was chosen. Protein treated samples were examined with a different filter set (excitation: BP 450–490 nm, filter block: 510 nm, emission: LP 515 nm), and a magnification of 10× was chosen for tests with BSA and 20× for tests with lysozyme. On every sample, 3–5 images were taken from each zone; this ensures that the obtained results were representative for the whole zone. Images within one JIP were always taken with the identical camera settings, i.e., using the same exposure time, gain and offset values. These images were evaluated with ImageJ by either counting the amount of fluorescent points (in case of NPs) or by measuring the average fluorescence intensity (in case of proteins).

2.10. Bacterial Adhesion Tests

Bacterial attachment to mucin coatings was evaluated for *S. aureus*, *S. pyogenes*, and *P. aeruginosa*. *S. pyogenes* strain ATCC 700 294 was cultured in Brain Heart Infusion Broth (Carl Roth), *S. aureus* USA300 in Lysogeny Broth (Carl Roth) supplemented with 0.1% dibasic potassium phosphate (Acros Organics) and *P. aeruginosa* PAO1 in pure Lysogeny Broth. The three strains were grown during shaking at 37 °C. Bacteria were directly diluted from overnight culture to an OD₆₀₀ of 0.2 (*S. aureus* and *S. pyogenes*) or grown to logarithmic phase (*P. aeruginosa*) and subsequently diluted to an OD₆₀₀ of 0.2. Bacteria were incubated under static conditions at 37 °C and 5% CO₂ for 1.5 h in wells containing uncoated or mucin-coated PDMS/PMMA

samples. Unattached bacteria were aspirated by removing the supernatant, and samples were washed with sterile PBS (1 mL) 1 to 4 times. Images were acquired at 20× magnification using the Zeiss microscope Primovert equipped with a Zeiss AxioCam ERc 5s. Adhesion of bacteria (*S. aureus*) or bacterial colonies (*S. pyogenes*) were quantified with the software ImageJ using the “find maxima”-command. The boxes for “exclude edge maxima” and “light background” were checked and the noise tolerance was set between 10 and 30 depending on the image. Images were preprocessed by adjusting brightness and contrast. If images were too noisy for a proper quantification, a gaussian smoothing algorithm (smoothing radius was set to 5.0 px) was applied to the images using the software gimp 2.8 (GNU Image Manipulation Program, The gimp team) prior to image analysis.

2.11. Fibroblast Adhesion

NIH/3T3 fibroblasts were maintained at subconfluency in T75 flasks with Dulbecco's modified Eagle medium (DMEM; Sigma-Aldrich) supplemented with 10% (v/v) fetal bovine serum (Sigma-Aldrich) and 1% (v/v) antibiotics solution (25 U mL⁻¹ penicillin, 25 µg mL⁻¹ streptomycin; both Sigma-Aldrich). The cells were detached using trypsin/EDTA (Sigma-Aldrich), and the cells were seeded at a density of 120 000 cells cm⁻² on uncoated and mucin-coated PDMS surfaces, respectively. After 24 h of incubation at 37 °C and 5% CO₂, the surfaces were washed twice with PBS. Cell viability was assessed by a live/dead assay employing a double-stain: 1 × 10⁻⁶ M calcein AM (Invitrogen, Carlsbad, CA, USA) and 2 × 10⁻⁶ M ethidium homodimer-1 (Invitrogen) were dissolved in serum free DMEM, and cells were incubated with this solution for 1 h before they were imaged on a DMi8 Leica microscope (Leica, Wetzlar, Germany) in fluorescence mode. Images were acquired with a digital camera (Orca Flash 4.0 C11440, Hamamatsu, Japan) using the software Leica Application Suite X (Leica).

2.12. Statistical Data Analysis

To detect significant differences between two examined groups, independent two-tailed *t* tests were conducted. Prior to testing, the normal distribution of the measured data was verified with the Shapiro-Wilk-test. Furthermore, the homogeneity of variances was tested using the F test. For non-normal distributed populations, the Wilcoxon-Mann-Whitney-test was used. For normal distributed populations with homogenous variances, Student's *t*-tests were performed, whereas a Welch's *t*-test was used in case of unequal variances. The software Prism 8 (GraphPad Software, San Diego, CA, USA) was used to conduct all statistical calculations. The level for significance was set to

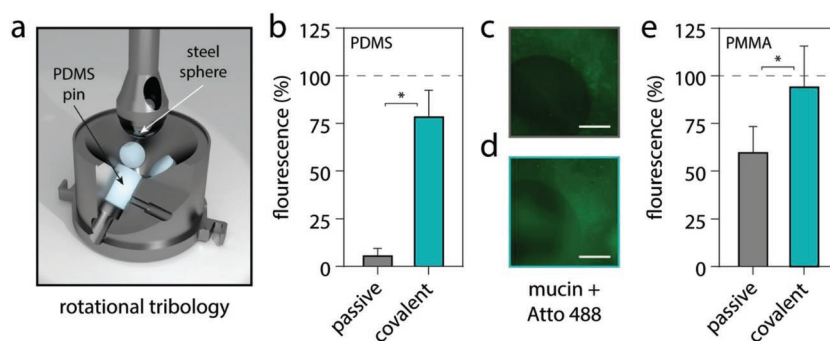


Figure 2. Mechanical stability of covalently coupled mucin coatings. a) Passively adsorbed and covalently linked mucin coatings are mechanically challenged using a rotational tribology setup. b) The ELISA signal obtained from tribologically treated mucin coatings is compared to that obtained from freshly coated samples (i.e., either passively and covalently coated ones, either are represented by the dashed line) that were not mechanically challenged. c,d) PDMS pins carrying coatings comprising fluorescently labelled mucins are imaged with fluorescence microscopy after they were subjected to tribological stress. c) Passively adsorbed mucins are sheared off in the circular contact zone whereas d) covalently linked mucins are still present in high numbers. Passively adsorbed and covalently linked mucin coatings generated on PMMA are exposed to an ultrasonic treatment. Mucins are also detected via ELISA, and the obtained signal is compared to freshly coated samples that were not challenged with ultrasound (dashed line). Error bars denote the standard deviation as obtained from $n = 9$ (b) and $n = 5$ (e) independent samples. The scale bars in (c) and (d) represent 1 mm.

$p < 0.01$, and significant differences between tested groups are marked with an asterisk in all graphs.

3. Results and Discussion

3.1. Stability of Covalently Coupled Mucins

Even though hydrophobic PDMS surfaces can be quickly and easily coated with mucins by means of passive adsorption, such a passively adsorbed mucin layer is not very stable: after exposure to mechanical shear forces, which here are applied by using a rotational tribology setup (Figure 2a, see the Experimental Section for details), most of the mucin coating is eroded (Figure 2b,c).

For a realistic medical application, e.g., the insertion of an endotracheal tube, such a loosely attached coating would be insufficient for several reasons. First, if the coating is sheared off from some areas of the PDMS surface, these uncoated surface spots are highly prone to protein deposition or bacterial adhesion. Second, if a medical device “releases” molecules (here: mucins) into the human body in an uncontrolled way, obtaining approval for this device becomes more difficult as all possible side effects related to this release need to be considered.^[22] Third, compared to mucin-functionalized surfaces, uncoated PDMS surfaces show inferior lubricity;^[5c,19] therefore, there will be a higher risk of tissue damage when a medical device, which has lost its coating, is removed again from the human body.

To overcome these problems associated with an insufficient mechanical stability of the coating, we investigate the performance of covalently coupled mucin coatings. We have demonstrated previously, how mucins can be covalently grafted onto a PDMS surface via a two-step coupling process: here, the PDMS

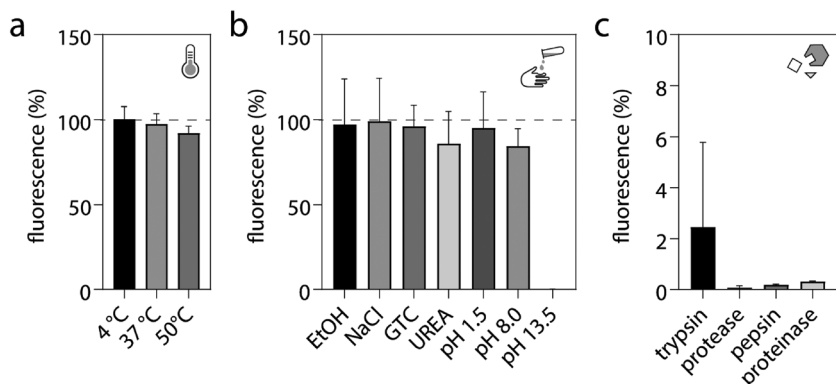


Figure 3. Thermal and chemical stability of covalently coupled mucin coatings. Mucin coatings generated on PDMS samples are exposed to a) different temperatures, b) selected chemical milieus (ethanol, chaotropic substances, high NaCl concentrations, and both, acidic and alkaline pH) as well as c) different proteolytic enzymes. The bars display the ELISA signal obtained after the thermal/chemical challenge and indicate the amount of intact mucins present on the PDMS samples in comparison to freshly coated but unchallenged samples (dashed lines). All error bars denote the standard deviation as obtained from $n = 3$ independent samples.

surface is first activated by oxygen plasma to prepare the surface for a silane-based precoating. Afterward, mucin glycoproteins can be attached to this silane layer via carbodiimide chemistry. To assess the mechanical stability of such a covalently attached mucin layer, we also expose this type of mucin coating to tribological shear stress by employing the same experimental procedure as described above. Indeed, both mucin detection methods (Figure 2b,d) demonstrate the very good stability of the covalent mucin coating, which drastically outperforms the stability of the passively adsorbed mucin layer. This is also indicated by the significantly higher amount of mucin molecules that remain after the tribological treatment (Figure 2b).

Of course, when used in the human body, medical devices are not only exposed to tribological shear stress but also to elevated temperatures of ≈ 37 °C. Moreover, during transport/shipping and storage of a medical device, the ambient conditions can vary and are not always precisely controlled. Thus, in a next step, we analyze the stability of our covalent mucin coating at three different storage temperatures, i.e., at 4, 37, and 50 °C. After overnight incubation at these different temperatures, we again assess the presence of mucins by ELISA tests and compare these results to freshly coated specimens. As depicted in **Figure 3a**, the amount of surface bound mucin remains stable after incubation and is hardly altered within the temperature range investigated here.

Since our covalent mucin coating shows promising results in terms of temperature resistance, we next test the stability of the coating after challenging it with different environmental conditions relevant for a putative medical application: First, as medical devices are often treated with ethanol (in the context of disinfection procedures) while handling them, we probe the stability of the mucin layer toward exposure to a high percentage (96%) EtOH solution. Interestingly, also here, the ELISA data shows, that the mucin layer is well resistant toward ethanol exposure (Figure 3b, see the Experimental Section for details).

In the human body, medical devices would always be exposed to physiological NaCl concentrations of $\approx 150 \times 10^{-3}$ M. Thus, in a next step, we analyze the stability of our coating toward the

influence of those salt ions. To maximize the putative impact such sodium and chloride ions could have, we expose our mucin coated samples to solutions containing 1 M of NaCl. However, even at those very high salt concentrations, the mucin coating again seems to be unaffected as the ELISA assay returns similarly high values as for unchallenged samples (Figure 3b).

One possible application of such mucin coatings would be to use them on urinary catheters; here, biofouling is a considerable issue. In the urinary tract, medical devices are constantly exposed to urea, a chaotropic substance. Chaotropic agents are able to reduce hydrophobic interactions, and such an effect may remove mucins from the PDMS surface that are not covalently attached but only passively adsorbed. Moreover, it may influence the conformation of surface-bound mucins and it can denature folded proteins if

present at high enough concentrations^[23]—and this could affect the detectability of our mucin coating via ELISA in case the oligopeptide epitope on the mucin terminus required for the antibody we use is compromised. However, even after exposure of mucin coated samples to a high concentration of urea (6 M solution) we do not find a significant reduction in the ELISA signal. Similar results are obtained when the even stronger chaotropic agent guanidinium thiocyanate (GTC, 1 M solution) is used to challenge the coating. Together, these tests further confirm that the mucins are indeed covalently attached to the PDMS surface and that denaturation of the (mostly unfolded) mucin glycoproteins plays a negligible role (Figure 3b).

Depending on the medical device the coating is supposed to be used on, also the pH of the tissue fluid the device gets in contact with can vary: (strongly) acidic conditions are relevant for medical devices to be used, e.g., in the stomach or the vaginal tract, and the small intestine exhibits a slightly alkaline pH around 8. To test the influence of this pH range, we also incubate some mucin coated samples in either 1 M formic acid (HCOOH, pH 1.5) or 1×10^{-6} M sodium hydroxide (NaOH, pH 8). Importantly, the former treatment does not affect the intensity of the ELISA signal at all, and the slightly basic pH only has a minor influence on the antibody-based mucin detection test. Strongly alkaline conditions, however, (as realized by a 1 M NaOH solution, pH 13.5) seem to fully remove or destroy the surface bound mucin layer (Figure 3b), probably by alkaline hydrolysis.^[24]

As a last group of physiologically relevant challenges, we investigate the influence of enzymatic degradation on the stability of the mucin coating. Proteolytic degradation of submaxillary bovine mucin by trypsin and pepsin has been investigated previously.^[25] Here, we expect the mucin coating to be somewhat vulnerable as not all parts of the mucin polypeptide chain are glycosylated thus leaving them exposed to enzymatic attack. Indeed, solubilized porcine gastric mucins are relatively resistant towards enzymatic degradation in their glycosylated areas, whereas the non-glycosylated terminal ends can be easily cleaved by trypsin.^[16] To challenge our mucin coating, we select

different variants of proteolytic enzymes: trypsin, protease type XIV, pepsin, and proteinase K. Trypsin naturally occurs in the small intestine and thus has its pH optimum between 7 and 9, whereas pepsin occurs in the stomach and has its optimum at pH values between 1.5 and 3. Protease type XIV is a mixture of enzymes and combines at least three caseinolytic activities with one aminopeptidase activity, and Proteinase K is a stable and highly reactive serine protease. The latter two enzymes exhibit their highest activity around neutral pH.

When our coating is exposed to any of those enzymes, we observe a strong reduction in the ELISA signal in each case (Figure 3c). Among all enzymes tested, the Proteinase K treatment has the weakest effect. Nevertheless, also here, a clear decrease of the ELISA signal is observed. However, due to the antibody assay used, it is difficult to directly correlate a reduced fluorescence signal obtained with ELISA with a loss of surface bound mucin. As mentioned above, the antibody used to detect mucin targets the polypeptide chain of the mucin molecule. Owing to the dense glycosylation pattern in the central region of the mucin glycoprotein, the polypeptide core is only accessible in the terminal regions of the macromolecule. Thus, enzymatic cleavage of these terminal regions could prevent the detection of the mucin via antibody staining although most of the molecule might still be present on the coated surface. To test this idea, we assess the functionality of the mucin layer after its exposure to an enzyme solution. The lubricity of such covalent mucin coatings has previously been shown to be a sensitive indicator for the coating quality.^[19] When mucin coated PDMS pins are tested in a rotational tribology setup, they reduce the friction between those pins and the counter surface: this effect is most pronounced in the mixed lubrication regime (where we detect a friction reduction by up to two decades) but still decent (reduction by >50%) in the boundary lubrication regime (Figure 4a, grey curve).

If such mucin coated pins are exposed to degrading enzymes such as trypsin, we find that the enzymatically challenged

mucin coating still shows a good lubricating performance—especially in the mixed lubrication regime. Only at very low sliding velocities, we observe a slightly increased coefficient of friction after enzymatic treatment (Figure 4a, cyan curve). Also, we again employ fluorescently labelled mucins to visualize the effect of trypsination. Compared to freshly coated PDMS samples, trypsinated specimens indeed show a reduced ELISA signal, however, this reduction is not significant (Figure 4b). Fluorescent images support this finding as they give a similar visual impression for both, samples with and without exposure to trypsin treatment (Figure 4c,d). From those experiments, we conclude that, indeed, trypsin does affect the mucin coating, and at least the exposed termini of the glycoprotein appear to be cleaved by the trypsin exposure. Furthermore, it is possible that—depending on the coating quality and density—also the surface bound termini of the attached mucins could be accessible for proteolytic enzymes.

3.2. Coating of Other Polymer Materials

Although silicone-based materials such as PDMS are very common for medical devices, there are many other polymer materials which are used in clinical applications (Table 1). For example, polyethylene (PE) is used in total joint replacements or as a material for catheters; polypropylene (PP) is often the basis for finger joint prostheses or non-degradable sutures; intraocular lenses, tooth replacements, and artificial tendons/ligaments are frequently made of polymethylmethacrylate (PMMA) or polyethylene terephthalate (PET); polyurethane (PU) and polyvinylchloride (PVC) are probably the most common materials for medical tubings, and PU is also used as a biocompatible, soft coating for titanium-based stents.

Since each of these polymers contains accessible hydrogen groups, they all can be activated by oxygen plasma in a similar manner as PDMS; thus, we expect that our two-step coating process can also be applied to those other medically relevant polymer materials. This is tested in the next step. Indeed, we can perform the mucin coating procedure on these six different polymer materials in very similar ways: Except for some minor changes in the process temperature (i.e., for all six additional materials, the temperature during the stabilization step is lowered to 60 °C—this requires an extension of this step duration to 4 h) and rinsing fluids (PMMA shows a poor resistance toward organic solvents; thus, those samples are cleaned with ultrapure water instead of EtOH and 2-propanol), the coating protocol is the same as described for PDMS specimens above. Afterward, as for the PDMS samples, we test the successful deposition of mucin by immunostaining.

For all coated polymeric materials, these ELISA tests return a significantly higher fluorescence signal compared to their uncoated counterparts (Figure 5a). This demonstrates that a considerable amount of mucin is

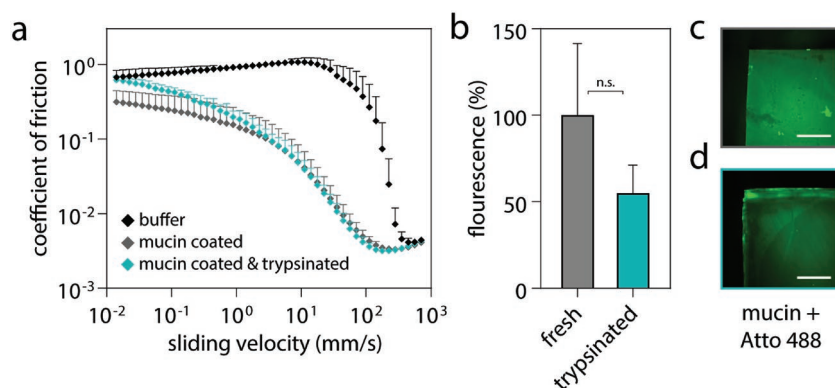


Figure 4. Effect of trypsin treatment on covalent mucin coatings. When probed with a steel sphere, the coefficient of friction obtained on uncoated PDMS samples (using 20×10^{-3} M HEPES as a lubricant) shows the typical shape of a Stribeck curve (black). Covalently coupled mucins on the PDMS surface reduce the coefficient of friction, especially in the mixed lubrication regime (grey). After exposure to a trypsin solution (cyan), the mucin coating performs similarly well as the unchallenged coating although experiments with fluorescently labelled mucins show a reduction in surface bound mucins after c,d) trypsin treatment compared to b,d) freshly coated samples (). Error bars depict the standard deviation as obtained from a minimum of $n = 3$ independent sets of PDMS samples.

Table 1. List of polymers used in this study. For each polymer, the table lists the full name and abbreviation, chemical structure of the respective monomeric unit, temperature limits of use, and typical medical applications.

Name	Monomer Structure	T_{max}	Medical Application
Polyethyl-methacrylate (PMMA)		75–80 °C	tooth fillings & replacements, intra-ocular lenses, bone cement ^[26]
Polyethylene-terephthalate (PET)		100 °C	artificial vessels, replacements for tendons & ligaments, surgical suture material ^[26a,27]
Polyvinyl-carbonate (PVC)		65 °C	tubings, catheters, blood pouches ^[26a,28]
Polyethylene (PE)		60–70 °C	medical containers, catheters, artificial tendons, total joint replacements ^[26a,27,29]
Polyurethane (PU)		80 °C	artificial cardiac valves, stent coatings, balloon catheters, tubings, vascular grafts, skin replacement, cardiac pace makers, long term implants ^[26a,29]
Polypropylene (PP)		100 °C	finger joint prosthesis, grafts, non-degradable sutures ^[27,29]
Polydimethyl-siloxane (PDMS)		200 °C	flexible and small joint replacements, breast implants, testicle implants, transfusion and catheter tubings, gastric bags, drains, endoscopic windows, bandages, contact lenses ^[26a,29]

present on all coated polymer surfaces. Since mucins are well hydrated and can bind a large amount of water molecules,^[30] we expect a mucin coating to render the surfaces of all polymeric substrates more hydrophilic. Experimentally this expectation can be tested by comparing the contact angle of mucin-coated materials to the values obtained from their uncoated counterparts. The contact angle is a frequently used indicator for analyzing the wettability of a surface and thus the surface energy: materials with a contact angle above 90° are considered hydrophobic, whereas materials with a contact angle below 90° are referred to as hydrophilic. Indeed, for all tested materials, the mucin coating entails a significant reduction in the contact angle—even the PDMS substrate, which shows an

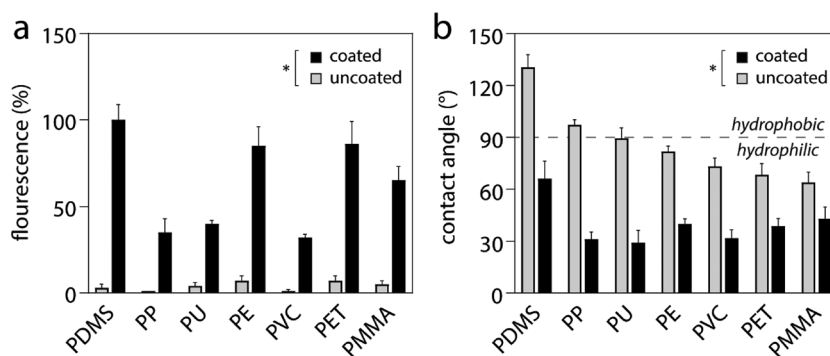


Figure 5. Covalent mucin coatings on different polymer materials. a) The presence of mucin on seven different medical polymer materials is verified via ELISA. b) Contact angle measurements compare the surface polarity of the polymer materials before and after mucin coating. The error bars depict the standard deviation as obtained from a minimum of $n = 3$ independent samples. As indicated by the asterisks in the two figure legends, the described properties of coated samples were always significantly different from their uncoated counterparts.

initial contact angle of $\approx 130^\circ$ (corresponding to a super-hydrophobic surface), is rendered hydrophilic after mucin functionalization (Figure 5b).

For PDMS samples, we have already shown above that the covalent coating procedure provides the mucin layer with good resistance toward mechanical stress. To confirm this finding for another polymeric substrate, we select PMMA, i.e., the polymer material with the most hydrophilic surface properties before coating. However, PMMA ($E_{\text{PMMA}} \approx 3 \text{ GPa}^{[31]}$) has a much higher stiffness than PDMS ($E_{\text{PDMS}} \approx 2 \text{ MPa}^{[32]}$); thus, the tribological test used for PDMS samples would generate a very high (and unphysiological) contact pressure that can easily induce wear on the PMMA substrate. Instead, we now chose an ultrasonic treatment as a gentler method to challenge the mechanical stability of the mucin coating on PMMA substrates. Indeed, this method is sufficient to reduce the surface fluorescence of the passively coated samples by $\approx 40\%$ indicating that a considerable amount of mucins is removed by the ultrasonic treatment (Figure 2e). In contrast, the covalently coupled mucin layer is virtually unaffected by the ultrasonic treatment as indicated by the significantly higher fluorescence signals obtained from those samples compared to passively coated ones.

3.3. Reduction of Particle and Protein Adsorption

So far, we have shown, that our covalent mucin coating is robust and resists both, mechanical stress and several physiologically relevant environmental challenges. Furthermore, one and the same coupling chemistry can be used to coat seven different polymer materials. In a next step, we aim at verifying that our covalently coupled mucin layer shows similar anti-fouling properties as reported previously for mucin coatings generated via passive adsorption. The following experiments are conducted with covalent mucin coatings generated on two different polymeric substrates. As for the mechanical stability tests, we again select PDMS as a relatively soft, hydrophobic substrate and PMMA, which is stiff but hydrophilic. Whereas quite different regarding their material properties, those two polymer materials are very suitable for the following investigations as they are both transparent thus allowing for optical microscopy tests in transmitted light mode.

First, we expose our mucin coatings to two types of polystyrene (PS) nanoparticles; the first variant exhibits a carboxylated surface and thus carries an overall negative charge ($\zeta_{\text{carboxy}} = -50.7 \pm 0.5 \text{ mV}$), and the second one exhibits an aminated surface resulting in an overall positive net charge ($\zeta_{\text{amine}} = +25.2 \pm 1.9 \text{ mV}$). When we analyze the amount of carboxylated particles adsorbed onto the different (uncoated versus coated) PDMS specimens via fluorescence microscopy, we observe a drastic reduction for mucin coated samples compared to uncoated PDMS (Figure 6a). For assessing the extent to which this effect is due to the mucin coating, we

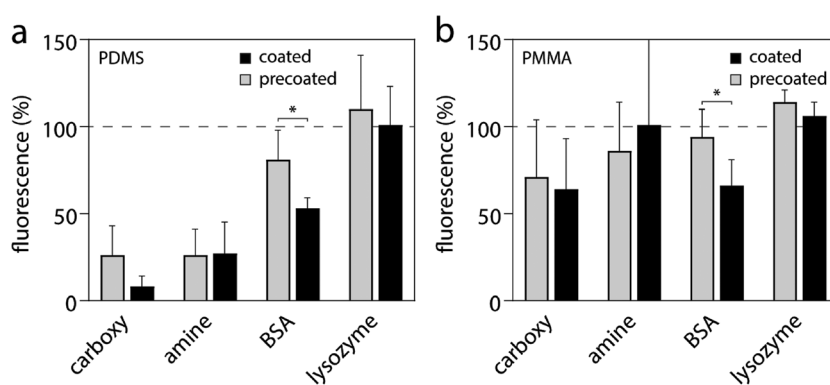


Figure 6. Protein and particle adsorption onto mucin coated surfaces. The adsorption behavior of carboxylated and amine-terminated polystyrene particles as well as BSA and lysozyme is determined for silane-precoatings and mucin coatings generated on a) PDMS or b) PMMA samples and compared to that obtained for uncoated specimens (horizontal lines in the respective subfigures). The error bars depict the standard deviation as obtained from $n = 3$ independent samples each.

also analyze PDMS surface carrying a silane pre-coating only; also here, much fewer particles are detected than on uncoated PDMS, yet more than on mucin coated specimens. This result is not really surprising as both, the silane pre-coating and the mucin coating, introduce a high density of negative charges onto the PDMS surface thus repelling the anionic PS particles through electrostatic repulsion. Since the deposition of large, polyanionic mucins onto the PDMS surface is likely to create stronger repulsive forces than the small, weakly charged silane, the higher efficiency of the mucin coating toward the anionic PS particle appears reasonable.

Interestingly, also adsorption tests with positively charged PS particles return a similar result (Figure 6a). This finding seems to challenge the idea that the mucin coating was to render the surface of the PDMS samples negatively charged—in this case, one would expect efficient adsorption of the cationic, amine-terminated PS particles. However, at this point it is important to recall that, at the buffer conditions used here, those amine-terminated PS particles exhibit a lower net charge than the carboxylated particles. Moreover, also carboxyl- or amine-terminated PS particles still exhibit a strongly hydrophobic character. Thus, we interpret our results such that—for the weakly charged amine-terminated PS particles—their adsorption behavior onto PDMS is dominated by hydrophobic interactions, and that weak, attractive electrostatic forces between the mucin coating and the PS particles are still preferable to the strong hydrophobic forces present for uncoated PDMS. Consequently, we expect the efficiency of the mucin coating to be less pronounced if the adsorption behavior of the same test particles is assessed on a hydrophilic substrate such as PMMA—and indeed, this is what we observe: for those specimens, the adsorption of anionic PS particles is reduced whereas the adsorption behavior of cationic PS particles is mostly unaffected (Figure 6b).

Of course, whereas giving mechanistic insight into the coating properties, polystyrene particles are a very crude model system for assessing anti-biofouling properties. Thus, in a second step, we now aim at testing the anti-adhesive properties of the mucin coating in a biomedically more relevant scenario.

As the process of biofouling always starts with the formation of a conditioning film, i.e., the uncontrolled adsorption of proteins, we tested the ability of our coating to reduce the adsorption behavior of both, a negatively and a positively charged model protein; accordingly, we selected fluorescent BSA (anionic at neutral pH) and lysozyme (cationic at neutral pH) as test molecules. Since neither of those well-folded proteins should carry a large number of hydrophobic amino acids on their surface, we expect that hydrophobic interactions should not play a major role regarding their adsorption behavior. In full agreement with this expectation, we find that the mucin coating returns comparable results on both materials, PDMS and PMMA: For the anionic BSA molecules, the mucin coating reduces the adsorption by $\approx 40\%$ and is significantly more efficient than the silane precoating alone; for the cationic lysozyme molecules, the adsorption behavior is comparable to the uncoated polymer materials (Figure 6a,b).

From those experiments we conclude that the mucin coating can very efficiently render hydrophobic materials resistant toward the adsorption of hydrophobic objects. Moreover, the mucin coating causes a significant reduction of the adsorption of anionic molecules on both, initially hydrophobic and hydrophilic materials.

3.4. Reduction of Prokaryotic and Eukaryotic Cell Adhesion

In the human body, the formation of a protein-based conditioning film on an artificial material is typically followed by

the colonization of bacteria or the encapsulation by fibroblasts. It has previously been shown, that passively adsorbed mucin coatings have repelling properties toward different (pathogenic) bacteria, e.g., *P. aeruginosa*, *S. epidermidis*, *S. aureus*, and *S. mutans*.^[7b,8,33]

We here first expose our mucin-coated surface to *S. aureus* bacteria. *S. aureus* does not cause infections in healthy individuals; however, in patients with a weakened immune system, this bacterium can lead to pneumonia, endocarditis or even sepsis. When an uncoated PDMS surface is incubated with a solution of planktonic *S. aureus* bacteria, a very large number of bacteria adsorbs to the surface. However, when the same bacteria are brought into contact with a mucin coated PDMS surface, the number of adsorbed bacteria is reduced by $\approx 35\%$ (this number represents the average reduction in adhered bacteria as obtained from $n = 3$ independent samples with $N = 3$ images each, see the Experimental Section for details) (Figure 7a). When the adhesion property of *S. aureus* is tested on PMMA surfaces, a qualitatively similar difference between coated and uncoated samples is observed (Figure 7b); however, now this difference is less pronounced ($n = 3$, $N = 3$). Next, we expose the two polymer materials to bacteria from the pathogenic strain *S. pyogenes*, which can, in addition to skin infections, be responsible for pharyngitis including severe forms of tonsillitis. Also here, light microscopy images of planktonic bacteria incubated on PDMS samples indicate, that the covalently coupled mucin layer can reduce bacterial adhesion to the polymer surface: we find an $\approx 35\%$ reduction on PDMS samples ($n = 3$, $N = 3$) and even a $\approx 62\%$ reduction on PMMA samples ($n = 3$, $N = 2$). As a

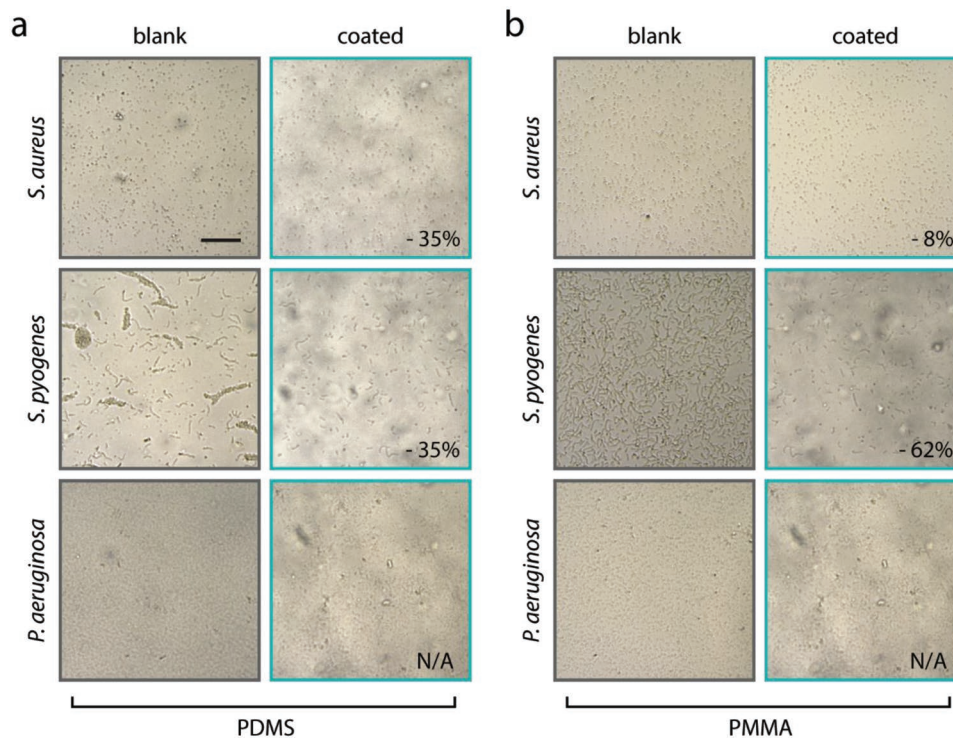


Figure 7. Covalent mucin coatings can reduce the surface colonization by selected bacteria. The adsorption of *S. aureus* and *S. pyogenes* onto PDMS and PMMA surfaces is reduced if a covalent mucin coating is applied previously to the bacterial exposure. *P. aeruginosa*, however, adheres similarly well to a mucin coated surface as to uncoated PDMS or PMMA surfaces. The scale bar represents 50 μm .

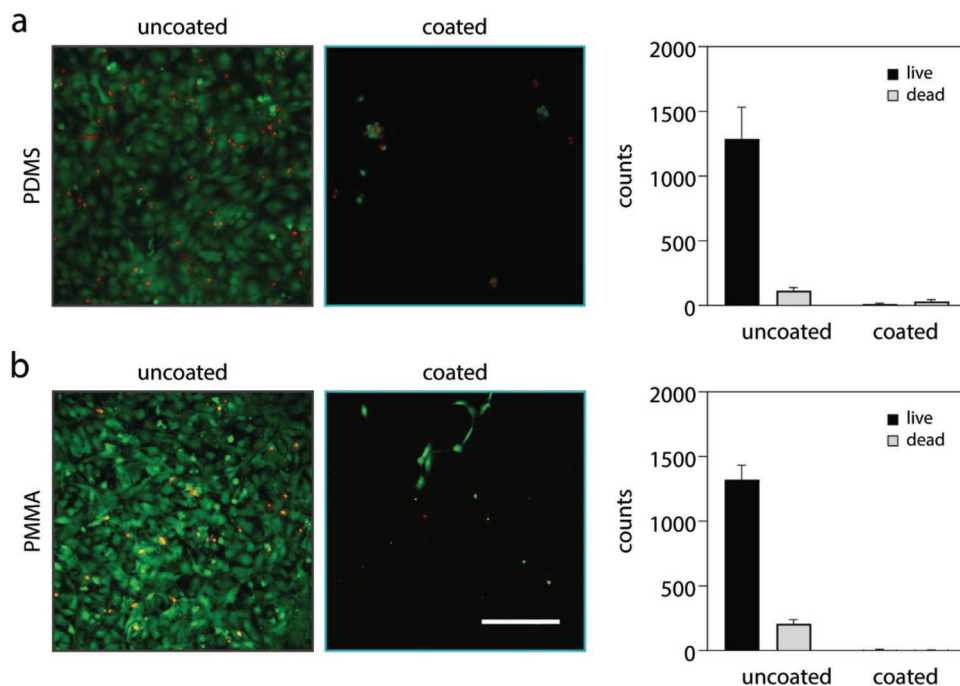


Figure 8. Covalent mucin coatings reduce fibroblast adhesion. The adsorption of NIH/3T3 fibroblasts onto both, PDMS and PMMA surfaces, respectively, is compared for uncoated samples and samples carrying a covalent mucin coating. The viability of the adsorbed cells is verified by performing a live (green signal)/dead (red signal) staining. Three images were analyzed per condition ($n = 3$). The scale bar represents 400 μm .

third pathogenic bacterium relevant in the context of biomedical devices we chose *P. aeruginosa*. Also *P. aeruginosa* is responsible for a multitude of nosocomial infections including pneumonia, skin infections or inflammations in the urinary tract. *P. aeruginosa* is a very resistant germ, that can survive in dry and humid conditions and has been shown to be mucoadhesive.^[34]

Consequently—as also shown before^[8]—those pathogens adhere very well to mucins, and we cannot observe a difference between coated and uncoated surfaces—neither on PDMS nor on PMMA substrates. (Figure 7a,b).

Having observed that mucin coatings can reduce the colonization of polymer surfaces by certain pathogenic bacteria, we next ask, if the antiadhesive properties of covalent mucin coatings also apply to eukaryotic cells. In detail, we assess fibroblast adhesion (see the Experimental Section for details) as an unwanted colonization of implanted materials is mostly responsible for fibrous encapsulation of implants. Fibrous encapsulation compromises the efficiency of the device and, on the long term, frequently leads to device failure. To test this, we here use an established fibroblast cell line (NIH/3T3 fibroblasts) which was already reported to not adhere to mucin coatings generated by simple passive adsorption.^[35] After incubation of those NIH/3T3 fibroblasts on uncoated and mucin-coated PDMS samples, respectively, we find that a confluent cell layer has formed on uncoated PDMS, whereas the amount of adsorbed fibroblasts on mucin-coated surfaces is very low (Figure 8). Additionally, the adsorbed cells on the respective surfaces differ in terms of their morphology: On uncoated PDMS, the fibroblasts exhibit their typical well-spread morphology indicating strong adhesion; on mucin-coated surfaces, however, the few adherent cells we find exhibit a relatively

round shape indicating weak adhesion. Still, we find that most of the cells adsorbed onto mucin-coated surfaces are still alive, which means that our mucin-coatings are not cytotoxic. Importantly, when we cultivate NIH/3T3 fibroblasts on uncoated and mucin-coated PMMA samples, respectively, we obtain a virtually identical result as on PDMS (Figure 8). This nicely illustrates that the ability of the covalent mucin coating to prevent fibroblast adhesion is independent from the carrier substrate the coating is generated on.

4. Conclusion and Outlook

In summary, we here demonstrated that our two-step coating process generates a stable mucin coating with anti-biofouling properties, which not only resists mechanical stress but is also very sturdy toward other physiologically relevant environmental conditions. Covalent mucin surface coatings as described here could be very useful for endotracheal tubings or urinal catheters, which are inserted into the human body and remain there for several days up to weeks—those devices are often prone to failure due to biofouling-induced inflammations. Furthermore, mucin coatings can also be a powerful tool for improving the lubricity of polymeric material surfaces^[19] and can help to reduce friction-induced damage on sensitive tissues.^[5c] By combining these different beneficial properties, mucin-based coatings should be highly interesting for a broad range of medical devices.

Statement of Ethics Approval

Approval of ethics is not required for the experiments conducted in this manuscript.

Acknowledgements

B.W. and M.G.B. contributed equally to this work. The authors thank Tobias Fuhrmann for assistance with the mucin purification and Theresa Lutz for conducting pilot experiments regarding the eukaryotic cellular adhesion.

Conflict of Interest

The authors declare no conflict of interest.

Author Contributions

B.W., M.G.B., M.M., and T.R. performed the experiments, which were designed by a combined contribution of all authors. B.W., M.G.B., and M.M. analyzed data, and B.W. and O.L. wrote the manuscript.

Keywords

bacterial adhesion, cell adhesion, friction reduction, protein adsorption, surface hydrophobicity

Received: December 9, 2019

Revised: December 19, 2019

Published online:

- [1] A. W. Bridges, A. J. García, *J. Diabetes Sci. Technol.* **2008**, 2, 984.
- [2] a) R. Konradi, B. Pidhatika, A. Mühlebach, M. Textor, *Langmuir* **2008**, 24, 613; b) Y. Wei, H.-C. Hung, F. Sun, T. Bai, P. Zhang, A. K. Nowinski, S. Jiang, *Acta Biomater.* **2016**, 40, 16.
- [3] a) I. Buzzacchera, M. Vorobii, N. Y. Kostina, A. de los Santos Pereira, T. Riedel, M. Bruns, W. Ogieglo, M. Möller, C. J. Wilson, C. Rodriguez-Emmenegger, *Biomacromolecules* **2017**, 18, 1983; b) K. A. Amoako, H. S. Sundaram, A. Suhaib, S. Jiang, K. E. Cook, *Adv. Mater. Interfaces* **2016**, 3, 1500646.
- [4] a) A. Roosjen, H. C. van der Mei, H. J. Busscher, W. Norde, *Langmuir* **2004**, 20, 10949; b) A. K. Muszanska, E. T. J. Rochford, A. Gruszka, A. A. Bastian, H. J. Busscher, W. Norde, H. C. van der Mei, A. Herrmann, *Biomacromolecules* **2014**, 15, 2019; c) M. R. Nejadnik, H. C. van der Mei, W. Norde, H. J. Busscher, *Biomaterials* **2008**, 29, 4117.
- [5] a) K. Chawla, S. Lee, B. P. Lee, J. L. Dalsin, P. B. Messersmith, N. D. Spencer, *J. Biomed. Mater. Res., Part A* **2009**, 90A, 742; b) C. Meng, *Science* **2009**, 323, 1698; c) B. Winkeljann, K. Boettcher, B. N. Balzer, O. Lieleg, *Adv. Mater. Interfaces* **2017**, 4, 1700186.
- [6] a) D. W. Branch, B. C. Wheeler, G. J. Brewer, D. E. Leckband, *Biomaterials* **2001**, 22, 1035; b) A. Roosjen, J. de Vries, H. C. van der Mei, W. Norde, H. J. Busscher, *J. Biomed. Mater. Res., Part B* **2005**, 73B, 347.
- [7] a) F. H. Labeed, R. P. Sear, J. L. Keddie, *Biofouling* **2010**, 26, 387; b) L. Shi, R. Ardehali, K. D. Caldwell, P. Valint, *Colloids Surf., B* **2000**, 17, 229; c) T. Sandberg, J. Carlsson, M. K. Ott, *Microsc. Res. Tech.* **2007**, 70, 864.
- [8] J. Y. Co, T. Crouzier, K. Ribbeck, *Adv. Mater. Interfaces* **2015**, 2, 1500179.
- [9] R. R. Janairo, Y. Zhu, T. Chen, S. Li, *Tissue Eng., Part A* **2014**, 20, 285.
- [10] R. Bansil, B. S. Turner, *Curr. Opin. Colloid Interface Sci.* **2006**, 11, 164.
- [11] H. J. Davidson, V. J. Kuonen, *Vet. Ophthalmol.* **2004**, 7, 71.
- [12] M. E. V. Johansson, H. Sjövall, G. C. Hansson, *Nat. Rev. Gastroenterol. Hepatol.* **2013**, 10, 352.
- [13] E. Lagow, M. DeSouza, D. Carson, *Hum. Reprod. Update* **1999**, 5, 280.
- [14] a) S. K. Linden, P. Sutton, N. G. Karlsson, V. Korolik, M. A. McGuckin, *Mucosal Immunol.* **2008**, 1, 183; b) M. A. McGuckin, S. K. Linden, P. Sutton, T. H. Florin, *Nat. Rev. Microbiol.* **2011**, 9, 265; c) M. Caldara, R. S. Friedlander, N. L. Kavanaugh, J. Aizenberg, K. R. Foster, K. Ribbeck, *Curr. Biol.* **2012**, 22, 2325.
- [15] L. Ma, A. Gaisinskaya-Kipnis, N. Kampf, J. Klein, *Nat. Commun.* **2015**, 6, 6060.
- [16] B. T. Käs Dorf, F. Weber, G. Petrou, V. Srivastava, T. Crouzier, O. Lieleg, *Biomacromolecules* **2017**, 18, 2454.
- [17] B. Winkeljann, A. B. Bussmann, M. G. Bauer, O. Lieleg, *Biotribology* **2018**, 14, 11.
- [18] a) K. Boettcher, B. Winkeljann, T. A. Schmidt, O. Lieleg, *Biotribology* **2017**, 12, 43; b) M. Biegler, J. Delius, B. T. Käs Dorf, T. Hofmann, O. Lieleg, *Biotribology* **2016**, 6, 12.
- [19] B. Winkeljann, P.-M. A. Leipold, O. Lieleg, *Adv. Mater. Interfaces* **2019**, 6, 1900366.
- [20] V. J. Schömig, B. T. Käs Dorf, C. Scholz, K. Bidmon, O. Lieleg, S. Berensmeier, *RSC Adv.* **2016**, 6, 44932.
- [21] a) J. Kim, M. K. Chaudhury, M. J. Owen, *J. Colloid Interface Sci.* **2000**, 226, 231; b) D. T. Eddington, J. P. Puccinelli, D. J. Beebe, *Sens. Actuators, B* **2006**, 114, 170.
- [22] ISO 10993-1:2018 Biological Evaluation of Medical Devices Part 1: Evaluation and Testing within a Risk Management Process.
- [23] G. D. Rose, P. J. Fleming, J. R. Banavar, A. Maritan, *Proc. Natl. Acad. Sci. USA* **2006**, 103, 16623.
- [24] P. Argüeso, M. Sumiyoshi, *Glycobiology* **2006**, 16, 1219.
- [25] J. B. Madsen, B. Svensson, M. Abou Hachem, S. Lee, *Langmuir* **2015**, 31, 8303.
- [26] a) E. Wintermantel, S. Ha, *Medizintechnik*, Springer, Berlin **2009**; b) W. Kaiser, *Kunststoffchemie für Ingenieure*, Carl Hanser Verlag GmbH Co KG, Munich **2006**.
- [27] G. Abts, *Kunststoff-Wissen für Einsteiger*, Carl Hanser Verlag GmbH Co KG, Munich **2016**.
- [28] W. Hellerich, G. Harsch, S. Haenle, *Werkstoff-Führer Kunststoffe*, Carl Hanser Verlag GmbH Co KG, Munich **1975**.
- [29] F. Puoci, *Advanced Polymers in Medicine*, Springer, Berlin **2015**.
- [30] T. Crouzier, K. Boettcher, A. R. Geonnotti, N. L. Kavanaugh, J. B. Hirsch, K. Ribbeck, O. Lieleg, *Adv. Mater. Interfaces* **2015**, 2, 1500308.
- [31] C. Ishiyama, Y. Higo, *J. Polym. Sci., Part B: Polym. Phys.* **2002**, 40, 460.
- [32] I. D. Johnston, D. K. McCluskey, C. K. L. Tan, M. C. Tracey, *J. Micromech. Microeng.* **2014**, 24, 035017.
- [33] E. S. Frenkel, K. Ribbeck, *J. Oral Microbiol.* **2015**, 7, 29759.
- [34] a) S. K. Arora, B. W. Ritchings, E. C. Almira, S. Lory, R. Ramphal, *Infect. Immun.* **1998**, 66, 1000; b) E. P. Lillehoj, B. T. Kim, K. C. Kim, *Am. J. Physiol.: Lung Cell. Mol. Physiol.* **2002**, 282, L751; c) A. Scharfman, S. K. Arora, P. Delmotte, E. Van Brussel, J. Mazurier, R. Ramphal, P. Roussel, *Infect. Immun.* **2001**, 69, 5243; d) M. S. Reddy, *Infect. Immun.* **1992**, 60, 1530.
- [35] T. Crouzier, H. Jang, J. Ahn, R. Stocker, K. Ribbeck, *Biomacromolecules* **2013**, 14, 3010.